Design and Testing of an Integrated Corn Stubble Residual Film-Recycling Machine

Le Wei [1], Xiaolong Liu [1,*], Wei Sun [1], Wuyun Zhao [1], Hui Li [1], Hua Zhang [1], Hongling Li [1], Jiadong Liang [2], Yongzhi Li [1], Yuhang Zhou [1] and Ningning Zhao [1]

[1] College of Mechano-Electronic Engineering, Gansu Agricultural University, Lanzhou 730070, China; wl1570738261@163.com (L.W.)
[2] Wuwei Xingdong Machinery Co., Wuwei 733000, China
* Correspondence: liuxiaol@gsau.edu.cn; Tel.: +86-189-1908-8968

Abstract: The existing residual film-recycling machines struggle to efficiently recover and separate film stubble in a single operation. With roller-type film-rolling device unloading difficulties and other problems, in order to improve the recovery efficiency of film stubble and the separation effect while reducing human labor and to improve work efficiency, we designed an automatic hydraulic unloading film stubble-recycling integrated residual film-recycling machine. The angle of the membrane lifting device was determined by theoretical calculations using the method of coupled simulation of EDEM and ANSYS Workbench. We analyzed the amount of resistance as well as the maximum stress and deformation during the working process of the membrane-lifting device and focused on the design of the membrane–soil separating device and membrane-rolling device. The depth of the film shovel, the forward speed of the machine, and the rotational speed of the driving wheel of the jogging chain were selected as the test factors, and the residual film recovery rate was taken as the evaluation index. A three-factor, three-level test was designed by applying the principles of the Box–Behnken experimental design. The results show that when the forward speed is 1.36 m/s, the soil depth is 147.16 mm, and the rotational speed of the driving wheel of the shaking chain is 77.89 r/min, the recovery rate of the residual film is 87.56%, and the relative error between the experimental value and the optimized value is 2.73%. The experimental results can provide a theoretical basis for the design of the residual film-recycling machine.

Keywords: residual film recycler; design; film-lifting mechanism; performance testing; optimization

1. Introduction

Mulching planting technology has the obvious effects of temperature increase, water conservation, moisture retention, and weed suppression, and is therefore commonly used in arid and semiarid areas [1,2]. China, as the country with the largest use of mulch, uses more than 1.5×10^6 t of mulch per year [3,4]. China's use of film is mainly based on polyethylene materials. In natural conditions, this film takes 200 to 400 years to degrade [5,6]. Residual used mulch in farmland damages the soil structure and reduces soil fertility, resulting in crop yield reduction, and the residual film itself also has a strong flexibility and is easy to entangle with the crop roots in the tillage layer, inhibiting the normal growth of crop roots [7]. There are a number of viruses and pests in the soil, and root stubble can be a breeding ground for them; if left untreated, this can have an impact on the crop afterward [8,9]. In recent years, with the increase in the area of mulching and the amount of film used, if not cleaned up in a timely manner, more and more film will be left in the soil of farmland, causing many problems for agricultural production and the ecological environment [8,10–12].

In recent years, for the planting of corn, cotton, potatoes, and other crops, the residual film-recycling machine pickup mechanism has been used with different structures, which

are mainly divided into shovel sieve type, drum type, bullet tooth type, toothed belt, and rake tooth type residual film-recycling machineries [13–17]. Mechanized residual film recycling plays an important role in environmental protection, but the current residual film-recycling machines have some problems in practical application, such as low recycling efficiency and a low degree of miscellaneous separation. In the process of the operation, residue will be entangled in the machine parts, which easily causes clogging damage, etc., to the equipment. In this paper, for the Gansu Hexi irrigation area, a corn land residual film-recycling machine is used for picking up film, unloading film, recycling stubble from coordinated operations, designing a set of film, picking up film, rolling film, unloading film, and recycling stubble with residual film-recycling equipment. By adjusting the height of the depth-limiting wheel, the machine makes the film-lifting device enter into the tillage layer. The shaking chain separates part of the soil in the film–stubble mixture from the gap of the chain bar. Most of the film is rolled up and recovered by the film-rolling device, and a small amount of broken film falls into the stubble box along with the root stubble, which can effectively recycle residual film and stubble in the tillage layer and reduce the amount of manpower needed. The corn stubble residual film-recycling machine designed in this paper is expected to contribute to solving the problems of environmental pollution and resource wastage existing in current agricultural production, promoting the sustainable development of agriculture, enhancing the economic benefits of farmers, and realizing the requirements of modern society regarding environmental protection and resource utilization.

2. Materials and Methods

2.1. Whole-Machine Structure

A corn stubble film-recycling machine mainly consists of a three-point suspension mechanism, a deceleration commutator, a film-starting device, a side film shovel, a chain drive system, a shaking delivery chain, a depth-limiting wheel, a film-rolling mechanism, a stubble collection box, and other parts of the structure of the machine, as shown in Figure 1. This machine is mainly used for the residual film-recycling operation after spring corn harvesting and straw crushing and returning to the field, and the operating parameters are shown in Table 1.
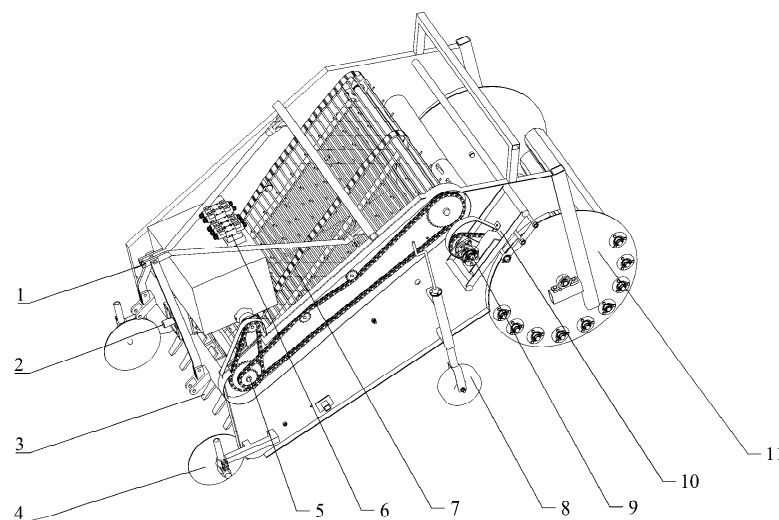

Figure 1. Whole-machine structure. 1. Three-point suspension mechanism. 2. Deceleration commutator. 3. Film starting device. 4. Side film shovel. 5. Chain drive system. 6. Hydraulic multiway valve. 7. Shake feeding chain. 8. Depth-limiting wheel. 9. Hydraulic motor. 10. Film-rolling device. 11. Stubble collection box.

Table 1. Main technical parameters of corn plastic film stubble recycling integration.

Parameters	Numerical Value
Size of the whole machine (mm × mm × mm)	3070 × 1920 × 1690
auxiliary power/kW	≥60
operating depth/mm	80~150
Working width/mm	1400
working speed (km·/h)	3.5~6

2.2. Principle of Operation

The integrated corn stubble residual film-recycling machine adopts a three-point suspension connection driven by tractor traction. When in operation, the implement moves forward under the tractor's pull. At the same time, the power output from the tractor's power output shaft is transferred to the chain drive device through the deceleration commutator. The chain drive device then drives the film–soil separating device, causing it to move. The membrane lifting device conveys a mixture of soil, residual film, stubble straw, and other materials from a soil depth of 150 mm. This mixture is lifted and transported by the nail teeth located on the chain bar of the film–soil separating device. During the conveying process, the shaking wheels on the film–soil separating device shake the surface soil, causing it to fall back to the ground. During transportation, the soil on the surface of the membrane is shaken by the shaking wheel of the membrane–soil separating device, which separates the soil and deposits it on the ground. A hydraulic motor drives the film rollers, causing them to rotate. As the residual film falls, it is pulled by the nail teeth of the film rollers, which wrap it around their surface due to their rotary movement. Under the force of gravity, the corn stubble and some straw fall into the stubble collection box. The stubble collection box drum then rotates to further separate the corn stubble from the soil. In addition, the stubble box is equipped with hydraulic cylinders on both sides that can be extended for easy unloading.

3. Design of Key Components

3.1. Design and Simulation of Membrane Lifting Device

3.1.1. Structure Design of the Stubble Lifting Spade

The film starting device works at a certain depth of film and crop stubble, and together, residual film and crop stubble and a small amount of straw in the field can be raised along the surface of the film shovel into a certain angle upward movement. Excess soil and fine impurities fall through the film starting device loosened in the gaps between the filtration. The actual working width of the film device is 1400 mm, with eight independent shovel bodies bolted to the square steel. The minimum gap is 85 mm. During the test, the spacing will not let the stubble out of the corn fall through the gap to the field. It can let the soil block pass through smoothly, and will not produce a soil clogging phenomenon. The film shovel surface and the ground are positioned at a certain inclination, to enhance the performance of the soil and to increase the efficiency of the machine on the residual film pick-up. This is shown in Figure 2.
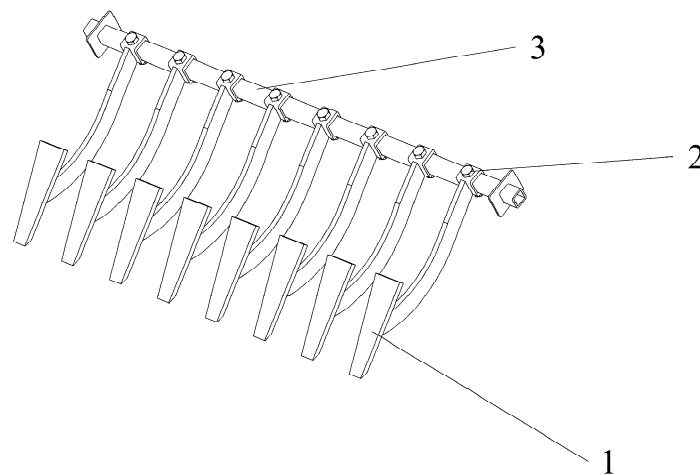
Figure 2. Film starting device. 1. Film stubble shovel. 2. Fixing screws. 3. Square steel.

3.1.2. Design of the Angle of Entry into the Ground

The film stubble shovel entry angle directly affects the efficiency of the machine. The force analysis of the shovel surface of the film and debris can be indirectly deduced from the theoretical value of the film shovel entry angle α, as shown in Figure 3.
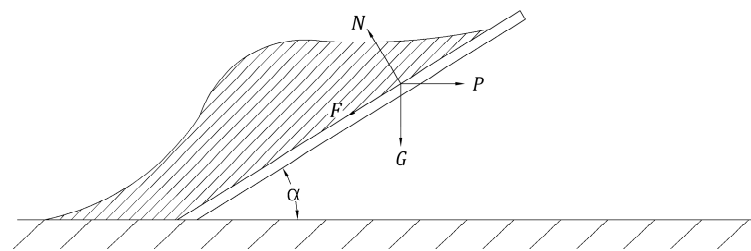

Figure 3. Stress analysis of film stubble shovel.

Since the film stubble shovel is not subjected to forces parallel to and perpendicular to the shovel surface, a balance equation can be established as follows:

$$P\cos a - F - G\sin a = 0 \tag{1}$$

$$N - G\cos a - P\sin a = 0 \tag{2}$$

$$F = \mu N \tag{3}$$

Here,
P—Working resistance of the film lifting shovel (N);
N—Pressure of the membrane mixture on the shovel surface (N);
G—Gravity of membrane mixtures on the shovel surface;
F—Friction of membrane mixtures on shovel surface;
μ—Friction factor between the shovel surface and the membrane-hybrid mixture.
These can be derived from Equations (1)–(3):

$$a = arc\tan \frac{P - \mu G}{G + \mu P} \tag{4}$$

From Equation (4), it can be concluded that if the angle of entry is too large, the film starting device may be congested with miscellaneous film mixtures on the surface of the shovel body in the process of moving forward, which will increase the working resistance; it was found in the test process that if the angle of entry is too small, the effect of crushing the soil will deteriorate, and the lifted film will be accompanied by a large amount of

soil with a large number of slabs, which will affect the separation of the miscellaneous film. According to the literature [18], the best effect of the film shovel is when the angle of entering the soil is 10~35°, and the final angle of film stubble shovel is $\alpha = 26°$, as deduced after many field experiments and discrete element simulation.

3.1.3. Simulation Analysis of Membrane Lifting Device

In the film starting device, for both the film and stubble functions, the material is 65Mn, and using the film starting device in the tillage layer will cause a certain resistance to the forward movement of the equipment. The resistance calculation is more complex and does not form a specific formula, mostly deduced from the test. For this reason, in this paper, based on the coupling of EDEM and ANSYS Workbench, the operational resistance of the membrane lifting device when working is derived in EDEM and imported into ANSYS for the static analysis of the membrane lifting device. The simplified processed membrane film starting device is shown in Figure 4. In order to make the simulation results more accurate, the simulation parameters were set according to the contact model of soil particles in the dry zone of Northwest China, studied by previous researchers [19–21], as shown in Table 2.
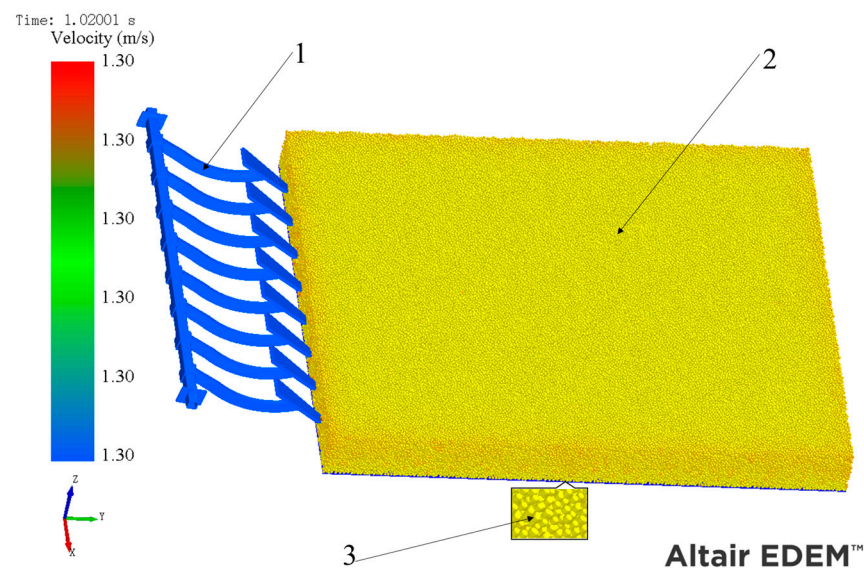

Figure 4. Virtual model of the membrane lifting device. 1. Virtual membrane lifting device. 2. Virtual soil trough. 3. Virtual soil particles.

We used SolidWorks to build a three-dimensional model of the film-starting device and import it into EDEM 2022.3 software in stl format, and set the geometric position and relevant contact parameters for it to simulate the force condition of the film starting device in the soil when it is working. In order to simplify the simulation model and reduce the simulation running time, the soil particles were set as spherical particles with a radius of 5 mm, and considering the adhesion between soil particles. It was more realistic to use the Hertz–Mindlin with JKR contact model, and the depth of soil penetration was determined to be 140 mm according to the literature on the distribution of maize stubble in various depths of the soil [22]. The simulation speed was set to be 1.3 m/s.

Post-processing of the discrete element simulation results was performed by coloring the soil particles with different colors for different speeds, observing the speeds obtained by the soil particles during the work of the film starting device, and then analyzing the motion of the soil particles, intercepting the speed of the soil particles over time, as shown in Figure 5.

Table 2. Discrete element simulation parameters.

Parameters	Numerical Value
Soil particle density/(kg·m^{-3})	2680
Poisson's ratio of soil particles	0.3
Soil particle shear modulus 0/Pa	1×10^8
65Mn steel density ρ/(kg·m^{-3})	7861
65Mn steel Poisson's ratio	0.29
65Mn steel shear modulus	7.9×10^{10}
Soil–soil recovery factor	0.3
Soil–soil kinetic friction factor	0.3
Soil–soil static friction factor	0.5
Soil–65Mn steel recovery factor	0.6
Soil–65Mn steel dynamic friction factor	0.11
Soil–65Mn steel static friction factor	0.4
JKR surface energy (J/m^2)	5.4
Dimensions of virtual soil tank (L × W × H)/mm × mm × mm	$2000 \times 1600 \times 200$
Advance speed of the film lifter m/s	1.3
Simulation time/s	3

1.1 s

2 s

2.9 s
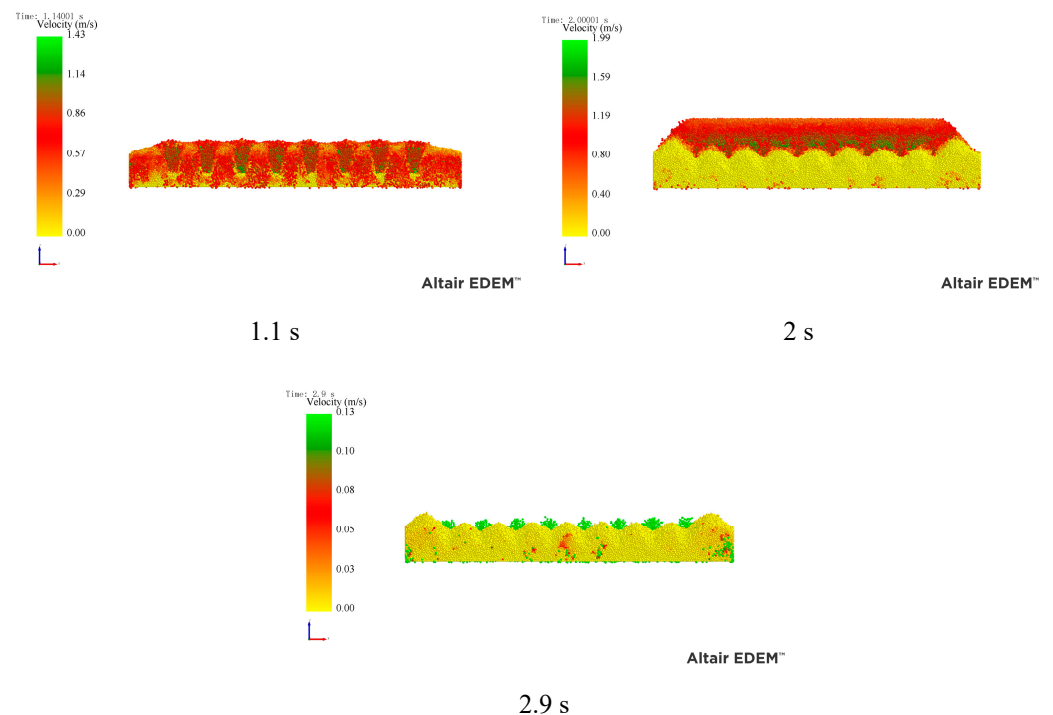
Figure 5. Soil particle velocity conditions.

Analysis of the speed of soil particles can be obtained. When the film device just is in the soil, the film device forward speed is similar to 1.43 m/s. When the film device is completely in the soil, the particles from the shovel surface along with the adjacent shovel blade gap are between the outflow, so that the speed increases to the maximum speed of 1.99 m/s. When the membrane lifting device completely leaves the soil, the velocity of the particles decreases obviously, but, due to the existence of inertia, there is still a small part of the soil with a certain velocity, and the rest of the particles have a velocity close to zero.

The simulation operation can be seen in Figure 6. In the process of advancing into the soil, the film starting device is in contact with the soil after 1 s. Through the post-processing function of EDEM software it can be seen that the maximum resistance suffered by the film starting device is 11,915.2 N, and the average resistance of the entire film-lifting device between 1 s in the soil and 2.2 s out of the soil is 9767.38 N.
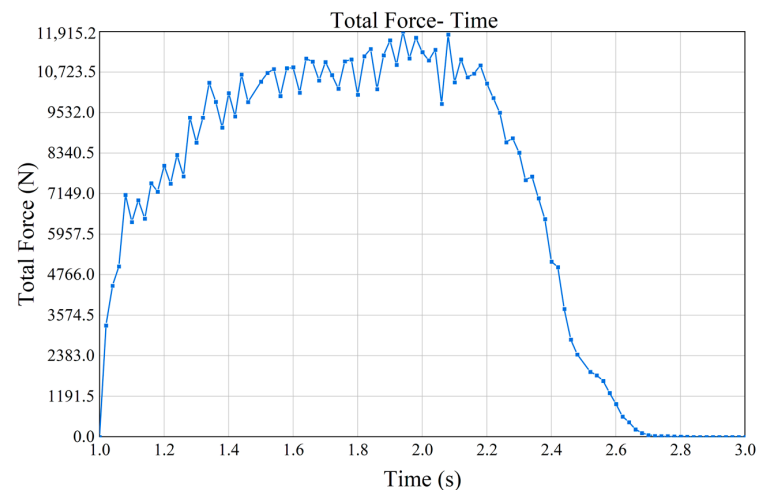
Figure 6. Film starting device resistance change curve.

After exporting the relevant files containing force data from EDEM, the stress–strain analysis can be carried out in ANSYS, and the coupling between EDEM and ANSYS is successful, as shown in Figure 7. After completing the coupling, the force data exported from EDEM are valid in ANSYS, and the deformation of the membrane film starting device is shown in Figure 8.
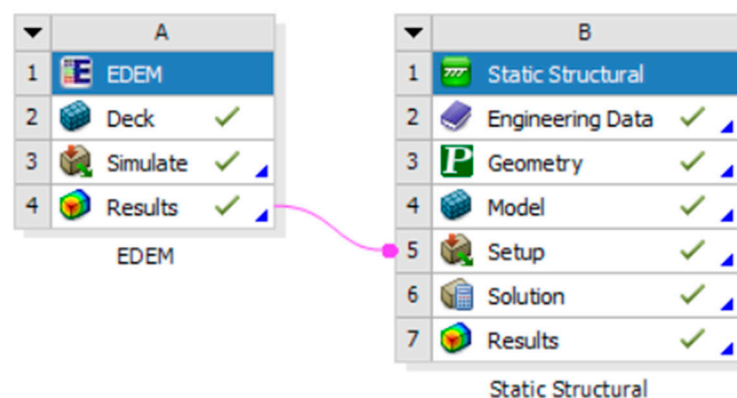

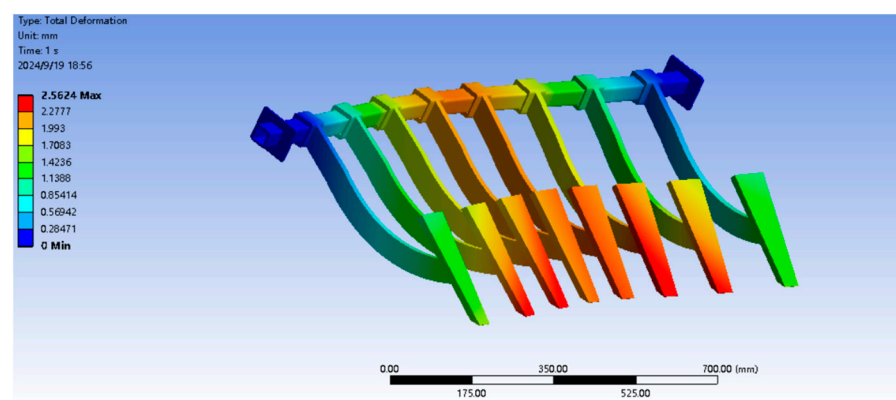**Figure 7.** Successful coupling interface.

Figure 8. Deformation of membrane device.

From the figure, it can be seen that the largest deformation of the film starting device is located in the position of the shovel tip, and the size of deformation is 2.56 mm, which is due to the fact that the shovel tip is always out of the deepest part of the soil in the

process of machine operation, and is subjected to the greatest resistance, which leads to the deformation of the film lifting device.

The stress distribution of the membrane film starting device when it is subjected to external load is shown in Figure 9.
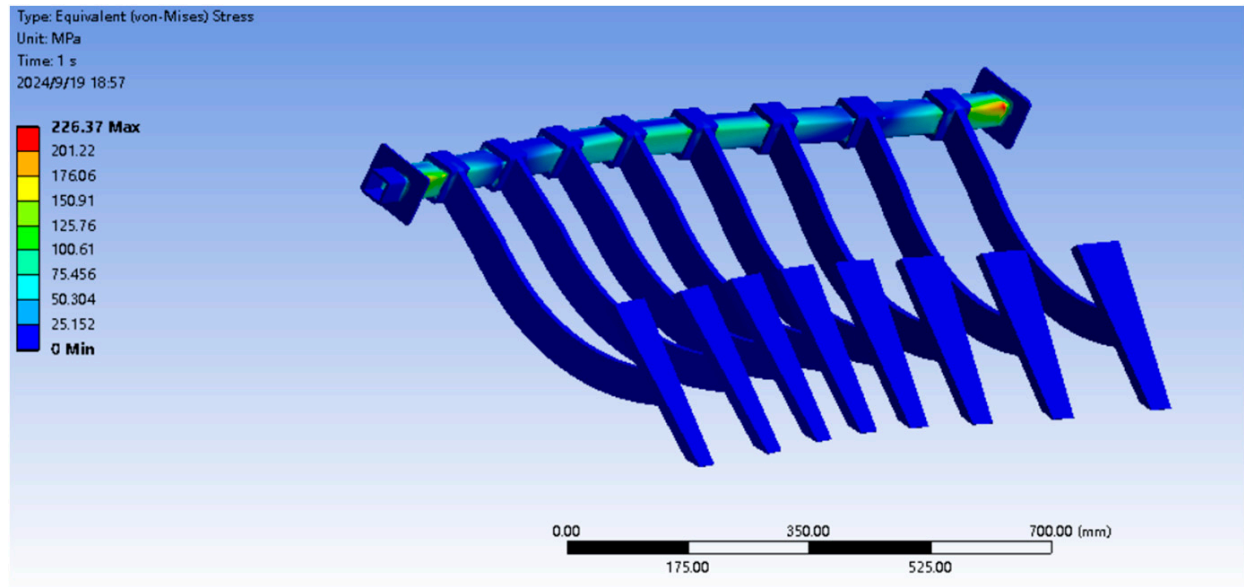

Figure 9. The stress distribution cloud diagram of the membrane device.

From the stress distribution cloud diagram of the film removal device, it can be seen that during the forward movement of the machinery, stress concentration occurs at the connection between the film stubble shovel and the square steel. The maximum stress value is 226.37 MPa, which is lower than the allowable stress of 65Mn, meeting the material strength requirements.

3.2. Design and Analysis of Membrane Soil Separation Unit

The membrane soil separation device mainly consists of a guide wheel, spike teeth, shaking delivery chain, hoisting wheel, drive wheel, and so on, and its structure is shown in Figure 10. The main function of the film–soil separator is to convey the film, stubble, and part of the straw shoveled up by the film-raising device to the film-rolling and stubble-collecting device. There are six spike teeth distributed on each chain bar on the shaking feed chain, and the distance between every two chain bars is 50 mm. There is a chamfer on the end surface of each spike tooth to ensure that the residual film and corn stubble will not be dislodged during the conveying process. The diameter of the driving wheel is 170 mm, and the shape of the shaking wheel is designed as an oval, which interacts with the shaking chain to produce a certain frequency of amplitude, in order to separate the soil, small straw and other impurities on the residual film. The residual film is rolled up by the film-rolling device along with the movement of the shaking chain to the highest place, and the root stubble and straw fall into the stubble box under the action of their own gravity, completing the whole film pickup work.
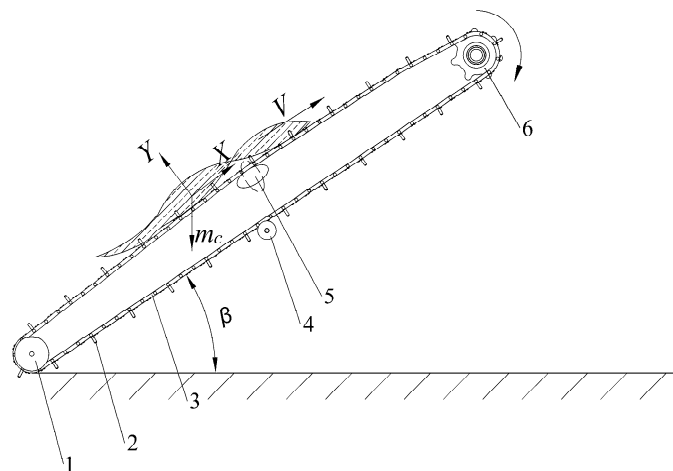
Figure 10. Structure diagram of film picking device. 1. Guide wheel. 2. Spike teeth. 3. Shaking delivery chain. 4. Hoisting wheel. 5. Vibrating wheel. 6. Drive wheel.

The installation inclination angle β of the shaking delivery chain in the membrane soil separation device is too large to make the residual film mixture slide downward under the action of gravity, and the installation inclination angle is too small to increase the length of the delivery chain, which increases the size and weight of the whole machine, so the installation inclination angle β of the delivery chain needs to be calculated by the force analysis to ensure that the value is reasonable. We take the root stubble straw residual film mixture as the research object to carry out force analysis.

$$m_c g \sin\beta \leq X \tag{5}$$

$$X = \mu_c Y \tag{6}$$

$$Y = m_c g \cos\beta \tag{7}$$

These can be derived from Equations (5)–(7):

$$\beta \leq \text{arctg}\,\mu_c \tag{8}$$

Here,
m_c—Mass of root stubble straw residue film mixtures (kg);
μ_c—Friction factor between the heterofilm mixture and the shaking chain;
X—Friction between the heterofilm mixture and the shaking chain, (N);
Y—Stress of heterogeneous membrane mixtures on the jogging chain, (N).

Based on subsequent field trials and the literature [23], it was determined that the best film pickup results were achieved when the jigger chain was installed with an inclination angle β of 30°.

3.3. Design and Analysis of Film Winding Device

3.3.1. Structural Design of the Film Winding Unit

The film-rolling device mainly consists of a hydraulic motor, left and right film-rolling rollers, opposite hydraulic cylinder group, film-rolling bullet teeth, film-rolling bracket, hanging lugs, guiding bushings, and hydraulic cylinders 1, 2, and so on, and its structure is shown in Figure 11a. When working, the hydraulic cylinder 1, 2 resets, then will roll the film elastic teeth out, then the hydraulic motor 1, 2 drive the chains and drive the left and right film roll rotation. When the left and right film roll on the residual film winding diameter reaches the maximum rotary diameter of the elastic teeth, we start to unload the film.
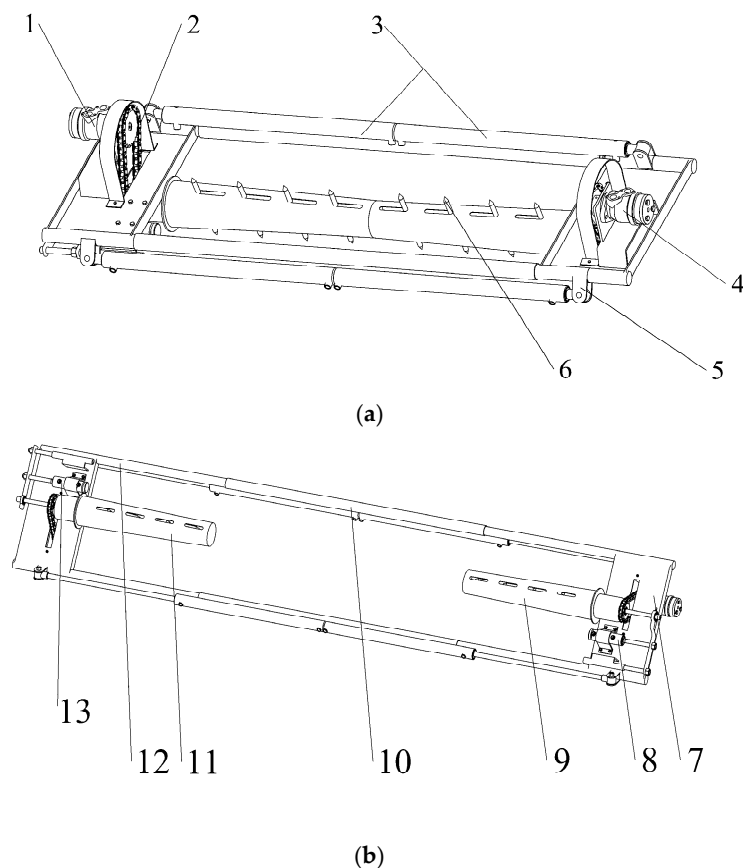
(**a**)

(**b**)

Figure 11. Structure diagram of film-rolling device. (**a**) Schematic structure of the rolled film state (**b**) Schematic diagram of the structure of the unloaded membrane state 1. Hydraulic motor 1. 2. Drive chain. 3. Opposite hydraulic cylinder group. 4. Hydraulic motor 2. 5. Lugs. 6. Film-rolling elastic teeth. 7. Film-rolling bracket. 8. Hydraulic cylinder 1. 9. Right film-rolling roll. 10. Guiding sleeve. 11. Left film-rolling roll. 12. Guiding shaft. 13. Hydraulic cylinder 2.

Determining how to unload the film quickly and saving labor in mechanized residual film recovery is a key link in the research, especially in the collection device with rotary winding residual film, which directly affects the working efficiency of the machine. In this paper, an automatic hydraulic film unloading device is designed based on the deficiencies in this link, as shown in Figure 11b. The guiding shaft sleeve and the two opposite hydraulic cylinders are fixed between the two side plates of the implement by welding. When the film rollers are wrapped with a certain amount of residual film, the film unloading area is stopped in the field, and the hydraulic cylinders control the elastic teeth on the left and right film rollers to retract. The guiding shaft is mounted inside the guiding shaft sleeve by clearance fit, and the guiding shaft is connected with the opposite hydraulic cylinders by the pin in the hole of the lugs, and the opposite hydraulic cylinder is stretched out when it is extended. When the opposite hydraulic cylinder group extends, the lugs drive the guiding shaft and then drive the components above the whole support to perform linear movement to both sides of the side plate of the implement. In this process, the side plate of the implement is equivalent to acting as scrapers, and the residual film wrapped around the film rollers is scraped down by the side plate to the designated film unloading area in the farmland.

3.3.2. Design of Rotational Speed of Film Rollers

In the normal operation of the machine, in order to make sure the residual film is smoothly wound to the film rollers, the film-rolling teeth have the role of backward pulling auxiliary winding. The speed of the film rollers directly affects the effect of the film. If the

speed is too low, the residual film is prone to falling off during the winding process; if the speed is too high, the residual film is likely to break and be stretched into strips, so we must design the speed of the film rollers.

The force analysis of the film-winding elastic teeth is shown in Figure 12. In order to ensure that the residual film does not fall off from the elastic teeth during the winding process, it is necessary to make the centrifugal force on the residual film less than the friction force, i.e.,

$$m_t g\left(cos\theta_1 + \frac{Rn^2}{g}sin\theta_2\right) \leq \mu_b m_t g(sin\theta_1 + \frac{Rn^2}{g}cos\theta_2) \tag{9}$$
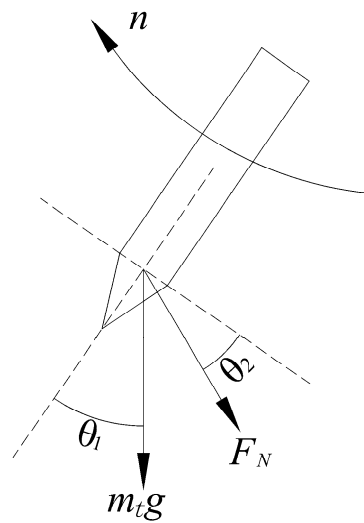

Figure 12. Analysis of the force on the teeth of the rolled film.

Here,

μ_b—Friction factor between the film reel teeth and the residual film;

m_t—Total residual film mass, (kg);

F_N—Inertial force on the residual membrane, (N);

R—Distance of the residual film on the tooth from the center of rotation of the tooth; (m)

θ_1—The angle between the direction of gravity and the teeth, (°);

θ_2—The angle between the inertial force on the residual film and the supporting force, (°).

In order to ensure that the residual film is not torn during the winding process, the force of the nail teeth on the residual film needs to meet the tensile strength of the residual film.

$$\frac{m_t(n\frac{dr}{dt})}{A} \leq [\sigma] \tag{10}$$

Here,

r—Radius of gyration of the tip of the tooth, m;

A—Contact area of the residual film with the elastic tooth, m^2;

$[\sigma]$—Permissible tensile force of residual film, MPa.

According to Equations (9) and (10), the working speed of the film rollers can be derived as

$$\sqrt{\frac{g(cos\theta_1 - \mu_b sin\theta_1)}{R(\mu_b cos\theta_2 - sin\theta_2)}} \leq n \leq \frac{[\sigma]Adt}{m_t dr} \tag{11}$$

From Equation (11), it can be seen that the rotational speed of the film winding roller is related to the angle of the film winding elastic teeth and the residual film performance. The

higher the allowable stress, the higher the working speed of the rollers, and the higher the efficiency of film rolling within a certain period of time. Tests have shown that the working speed of the rollers is 120~150 rad/min, which is the best for film rolling [24].

3.4. Design of Self-Loading Stubble Collectors

The self-discharging stubble collection device is located in the back of the residual film-recycling machine, mainly composed of a side plate, rotating roller, frame, hydraulic cylinder, bearing with seat, sprocket and other components. Its structure is shown in Figure 13.
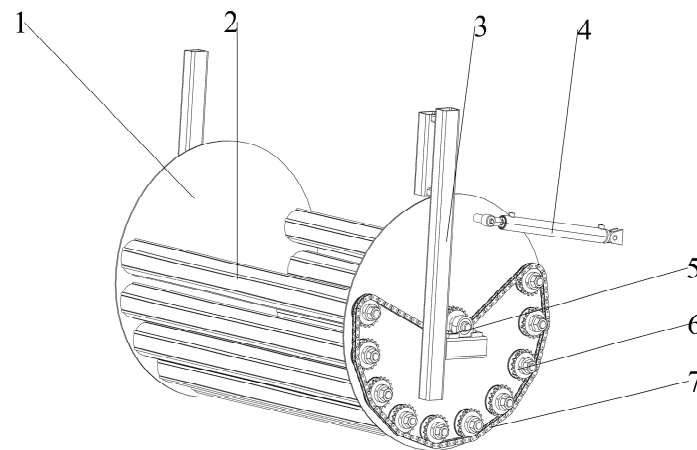

Figure 13. Schematic diagram of the structure of a stubble collection box. 1. Side plate. 2. Rotating roller. 3. Frame. 4. Hydraulic cylinder. 5. Seated bearing. 6. Sprocket. 7. Chain.

The rotating roller realizes isotropic rotation through the chain drive. When working, the crop stubble separated by the shaking and sending chain falls into the stubble box. The rotating roller rotates and drives the crop stubble to roll repeatedly in the stubble box, further separating the soil attached on the stubble. The separated soil falls down from the gap of the rollers, further completing the separation and ensuring that the organic matter in the soil is not wasted. When the amount of crop stubble reaches a certain level, the hydraulic multiway valve is controlled so that the hydraulic cylinder extends, driving the stubble collection box rotation and the crop stubble unloading.

4. Results

4.1. Test Conditions

The test site was selected as a spring harvested corn field at the test base of Gansu Agricultural University in Wuwei City, Gansu Province. The terrain of the test field was relatively flat, and the soil type was sandy soil. The average moisture content of the surface soil was 9.79%, and the film thickness was 0.01 mm. A Dongfanghong tractor with a rated power of 90 kW was used as the supporting power. The main test equipment included a 60-m tape measure, an electronic balance scale with an accuracy of 0.01 g, a stopwatch with an accuracy of 0.01 s, and a tachometer. The field operation of the machine is shown in Figure 14.

Figure 14. Field test of operation performance of residual film-recycling machine.

4.2. Test Factors and Test Indicators

According to the structure and operating parameters of the integrated corn stubble recovery machine, three key parameters affecting the pickup effect were selected as the main influencing factors of this test. According to the previous theoretical analysis and the expected test, the forward speed X_1, the depth of soil entry X_2, and the rotation speed of the driving wheel of the shaking delivery chain X_3 were selected as the influencing factors to carry out the response surface experimental research, and the residual film recovery rate Y_1 was selected as the response value according to the actual situation in the field. The test factors and levels are shown in Table 3.

Table 3. Factors and levels of experiment.

Levels	Moving Speed $v/(\text{m·s}^{-1})$	Depth into Soil $h·\text{mm}^{-1}$	Jitter Conveyor Chain Drive Wheel Speed $n/(\text{r·min}^{-1})$
−1	1	80	60
0	1.3	115	90
1	1.6	150	120

The test was designed with reference to the provisions of the GB/T 25412-2021 [25] residual film-recycling machine. Seventeen areas in the field were selected as experimental zones, each of which was 50 m in length, and five sample collection points of 1 m² in size were arbitrarily selected within each experimental zone. Before the test, the residual film within 150 mm below the surface was collected, cleaned, and dried, and then weighed, and the average value of M_1 (g) was recorded for each group. After the completion of the test, the residual film was collected within the depth of 150 mm of the plow layer, and the test samples were cleaned, dried, and weighed, and the average value M_2 (g) was recorded for each group of values. The ratio of the values measured before and after the test gives the residual film recovery rate η (%) as follows:

$$\eta = (1 - \frac{M_2}{M_1}) \times 100\% \tag{12}$$

4.3. Test Results and Analysis

4.3.1. Test Results

A three-factor, three-level test was designed according to the principles of the Box–Behnken test, and the design scheme of the test as well as the results of the test response values are shown in Table 4.

Table 4. Experimental scheme design and response value.

Number	Moving Speed X^1	Depth into Soil X^2	Jitter Conveyor Chain Drive Wheel Speed X^3	Rate of Recovery Y/%
1	1	0	−1	86.15
2	0	1	1	82.62
3	−1	1	0	85.79
4	0	1	−1	86.25
5	0	−1	−1	82.20
6	0	−1	1	79.05
7	0	0	0	85.77
8	0	0	0	86.05
9	1	−1	0	83.68
10	−1	0	1	79.31
11	−1	0	−1	82.81
12	1	1	0	85.95
13	0	0	0	86.87
14	0	0	0	86.29
15	−1	−1	0	80.41
16	1	0	1	80.79
17	0	0	0	85.93

4.3.2. Experimental Regression Analysis

Based on the data samples in Table 4, the multiple regression fitting analysis was performed by Design-Expert software to find the optimal solutions of the parameters. The experimental results in Table 4 were analyzed by ANOVA and shown in Table 5. The recovery in the response surface model Y_1 had a $p < 0.0001$, which indicates that the regression model is highly significant. The misfit term $p = 0.361$ indicates that the regression equation has a high degree of fit; its coefficient of determination R^2 is 0.9871, which indicates that this data model can explain more than 98% of the evaluation indicators. Therefore, the working parameters of this machine can be optimized by this model.

Table 5. Variance analysis of regression equation.

Source	Recovery Rate of Residual Film			
	Sum of Squares	Degree of Freedom	F	Significant Level
Model	115.81	9	59.34	<0.0001 **
X_1	8.51	1	39.23	0.0004 **
X_2	29.15	1	134.40	<0.0001 **
X_3	30.58	1	140.99	<0.0001 **
X_1X_2	2.42	1	11.15	0.0124 *
X_1X_3	0.86	1	3.99	0.0860
X_2X_3	0.058	1	0.27	0.6222
X_1^2	6.52	1	30.08	0.0009 **
X_2^2	4.04	1	18.64	0.0035 **
X_3^2	30.07	1	138.64	<0.0001 **
Residual	1.52	7		
Lack of fit	0.78	3	1.42	0.3610
Pure error	0.74	4		
Total	117.33	16		

Note: $p < 0.01$ (highly significant, **); $p < 0.05$ (significant, *).

The optimized regression equation is obtained by removing the insignificant regression terms in the model:

$$Y_1 = 86.18 + 1.03X_1 + 1.91X_2 - 1.96X_3 - 0.78X_1X_2 - 1.24X_1^2 - 0.98X_2^2 - 2.67X_3^2$$

4.4. Analysis of the Influence of Interaction Factors on the Working Performance of the Machines

According to the results of the regression equation analysis, 3D-surface response surface plots were drawn using Design-Expert 8 software, and the effects of forward speed, depth of penetration, and rotation speed of jogging chain drive wheels on the recovery

rate Y_1 are shown in Figure 15. The influence effects of the three influencing factors were jogging chain driving wheel speed > depth of entry > forward speed. Figure 15a shows the surface plot of the interaction response between the forward speed of the implement and the depth of entry on the recovery rate for a determined speed of the drive wheel of the jitter feed chain. As can be seen from the figure, with the increase in the forward speed and the depth of the soil, the residual film recovery rate first rises sharply and then gradually tends to stabilize. This is due to the fact that it is not possible to lift part of the residual film below the surface of the ground when the film lifting device is at a shallow depth. The residual film below the surface can be shoveled up when it reaches a certain depth, and, thus, the recovery rate stabilizes. From Figure 15b, it can be seen that for a defined depth of entry, the recovery rate first increases and then levels off as the forward speed increases. As the rotational speed of the jigger chain drive wheel increases, the recovery rate first rises and then falls sharply; this is because the higher the rotational speed of the driving wheel, the higher the linear speed of the shaking chain. Too high a linear speed will cause the residual film by the chain rod to be shredded on the nail teeth. Shredded residual film is not easily rolled up by the machine's film-rolling device; a part of the residual film will fall into the film miscellaneous box, and the other part of the residual film will drift to the farmland, bringing about inconvenience. Figure 15c shows the impact of the interaction response between the depth of entry and the rotational speed of the jogging chain drive wheel on the residual film recovery rate. When determining the forward speed, the residual film recovery increases with depth of penetration, and when the depth of the soil is about 130 mm, the growth rate of the recovery rate tends to flatten out. The drive wheel speed first rises and then falls sharply, which indicates that the drive wheel speed cannot be too high or too low. When it is too high, the nail teeth will tear the residual film, and the film miscellaneous mixtures stay in the chain tooth mechanism for too short a period of time. This cannot be effective in the screening and separation. If the shaking delivery chain line speed is too low, there will be a congestion phenomenon, which will increase the forward resistance.
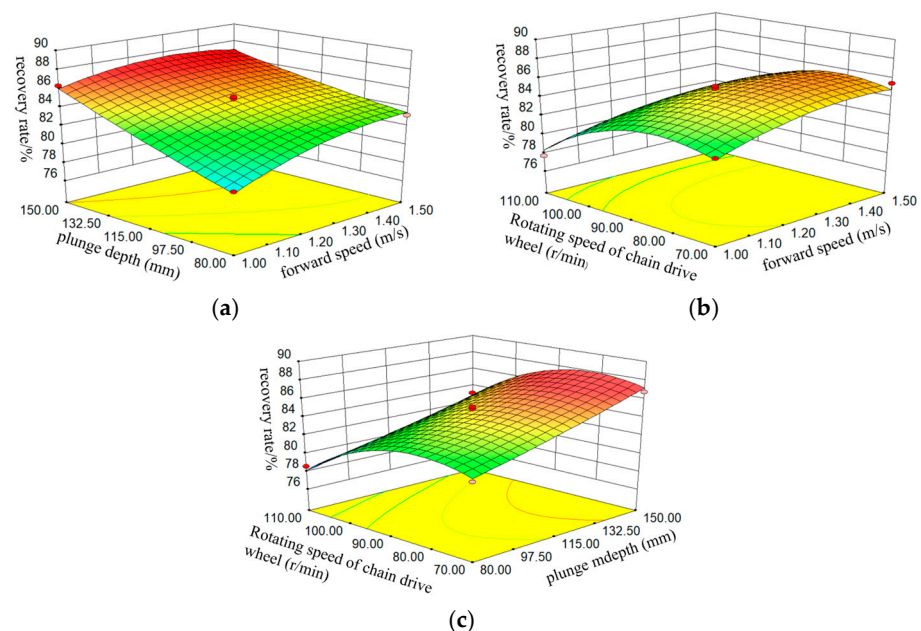

(a)

(b)

(c)

Figure 15. (**a**) Surface plot of forward speed and plunge depth of entry response. (**b**) Surface plot of forward speed and rotating speed of chain drive wheel speed response. (**c**) Surface plot of plunge mdepth and rotating speed of chain drive wheel speed response. Response surface diagram of the influence of various factors on the recovery rate of residual film.

4.5. Parameter Optimization and Experimental Validation

To achieve the best performance of the machine, it is necessary to optimize the influencing factors in the test. Based on the analysis of the orthogonal test results, these factors were chosen to obtain the optimal combination: a forward speed of 1.36 m/s, a soil entry depth of 147.16 mm, and a chain drive wheel shaking speed of 77.89 r/min. At this point, the residual film recovery rate reached 87.558%.

To verify the accuracy of the optimization results, three replicated experiments were conducted in the experimental area of Gansu Agricultural University in Wuwei City, Gansu Province, China. Based on the previous results and considering the feasibility of the field test, the forward speed was set to 1.4 m/s according to the tractor gear. The transmission ratio was adjusted by replacing the sprocket wheel to change the rotational speed of the shaking chain's drive wheel, which was ultimately determined to be 80 r/min. The depth of entry was controlled by adjusting the height of the depth-limiting wheel. According to the response surface analysis, when the depth of entry is approximately 140 mm, the recovery rate tends to stabilize. A deeper entry would increase the forward resistance of the machine; therefore, the depth of entry was set to 140 mm for the test, and the results are shown in Table 6.

Table 6. Optimization results and experiment verification results.

Sports Event	Residual Film Recovery Rate/%
Test average	84.83
Optimal value	87.56
Relative error	2.73

Through this analysis, it can be seen that the relative error between the average value of experimental verification and the theoretical optimization value is less than 5%, which proves that the optimization of parameters is reliable. The average recovery rate of residual film is measured to be 84.83% when the forward speed of the machine is 1.4 m/s, the depth of entry into the soil is 140 mm, and the rotation speed of the jogging chain driving wheel is 80 r/min during the operation of the machine on field.

5. Conclusions

(1) We designed a residual film-recycling equipment that can complete a series of operations such as film lifting, film pickup, film rolling, film unloading, etc., and realize film stubble recycling and separation. The design parameters of the film lifting device and film soil separation device were determined.

(2) We took the forward speed of the machine, the depth of the soil, and the rotational speed of the driving wheel of the shaking feed chain as the test factors, and took the residual film recovery rate as the index to carry out the test. We used the Design-Expert software to carry out the response surface analysis on the test results, and the results show that the order of the influence of each factor on the residual film recovery rate is as follows, from large to small: the rotational speed of the driving wheel of the shaking feed chain, the depth of the soil, and the forward speed.

(3) Using the data optimization function of Design-Expert software, with the residual film recovery rate as the optimization objective, the best working parameters were determined as follows: the forward speed was 1.36 m/s, the depth of entry was 147.16 mm, the rotational speed of the driving wheel of the jogging chain was 77.89 r/min, and the residual film recovery rate was 87.56%. The field test was carried out after the parameters were adjusted according to the actual conditions of the machine and the limitations of the transmission system, and the results of the field test showed that the recovery rate of the residual film was 84.83%, and the relative error between the average value of the test and the optimized value of the result was 2.73%, which was less than 5%, indicating that the model reliability was relatively high.

(4) In this paper, the experiment was carried out on the maize field that had been harvested in the spring at the experimental base of Gansu Agricultural University in Wuwei City, Gansu Province, but there were some shortcomings due to the limitations of the weather and testing conditions. The limitations and influences of the climatic conditions and the harvesting time, such as fluctuations in the temperature, rainfall, and illumination, may lead to uncertainty of the experimental results. The machine's operating trips were short, the data samples collected were small, and only the theoretical operating productivity was determined. The implements in this trial and the manufacturers will work closely together and will gradually carry out demonstration and promotion activities in a number of regions in order to enhance the adaptability and reliability of the implements.

Author Contributions: Conceptualization, L.W., X.L., W.S., and H.L. (Hui Li); data curation, L.W.; formal analysis, L.W.; funding acquisition, X.L.; investigation, L.W., Y.L., and Y.Z.; methodology, L.W., W.Z., H.Z., and H.L. (Hongling Li); project administration, X.L.; resources, L.W. and J.L.; software, L.W.; supervision, X.L.; validation, L.W. and N.Z.; writing—original draft, L.W.; writing—review and editing, L.W. and X.L. All authors have read and agreed to the published version of the manuscript.

Institutional Review Board Statement: Not applicable.

Data Availability Statement: Data are reported within the article.

Conflicts of Interest: Author Jiadong Liang was employed by the Wuwei Xingdong Machinery Co. All authors declare that the research was conducted in the absence of any commercial or financial relationships that could be construed as potential conflicts of interest.

References

1. Hu, Q.; Li, X.; Shi, H.; Chen, N.; Zhang, Y.; Ma, H. Response of Corn Root System to Residual Film and Root Distribution Model in Hetao Irrigation Area. *Agric. Eng. J.* **2021**, *37*, 143–152.
2. Liang, R.Q.; Chen, X.G.; Zhang, B.C.; Meng, H.; Jiang, P.; Peng, X.; Kan, Z.; Li, W. Current Issues and Strategies for Residual Film Recovery and Resource Utilization in Xinjiang Cotton Fields. *Agric. Eng. J.* **2019**, *35*, 1–13.
3. Hu, C.; Wang, X.F.; Chen, X.G.; Tang, X.; Zhao, Y.; Yan, C. Current Status and Prevention Strategies of Residual Film Pollution in Xinjiang Farmland. *Agric. Eng. J.* **2019**, *35*, 223–234.
4. Wang, Z.C.; Meng, Q.; Yu, L.H.; Yang, W.; Li, W.; Yang, J.; Yang, F. Characteristics of Microplastics in Agricultural Soils of Inner Mongolia Hetao Irrigation Area. *Agric. Eng. J.* **2020**, *36*, 204–209.
5. Yan, C.R.; Liu, E.K.; Shu, F.; Liu, Q.; Liu, S.; He, W. Characteristics and Control Technology of Plastic Film Coverage and Residue Pollution in China. *J. Agric. Res. Environ.* **2014**, *31*, 95–102. [CrossRef]
6. Sun, Y.; Jian, J.M.; Tian, Y.T.; Sun, F.; Zhang, M.; Wang, S. Analysis and Experiment of the Mechanism of Rotating Film Removal Device for Residual Film Recovery. *J. Agric. Mech.* **2018**, *49* (Suppl. S1), 304–310.
7. He, W.Q.; Yan, C.R.; Liu, S.; Chang, R.; Wang, X.; Cao, S.; Liu, Q. Research on Application and Pollution Status of Plastic Film in Typical Cotton Regions. *J. Agric. Environ. Sci.* **2009**, *28*, 1618–1622.
8. Wang, L.; Lin, T.; Yan, C.R.; Wang, J.; Guo, R.; Yue, L.; Tang, Q. Effects of Residual Film Amount on Evapotranspiration and Inter-Row Evaporation in Xinjiang Cotton Fields. *Agric. Eng. J.* **2016**, *32*, 120–128.
9. Wang, Z.H.; He, H.J.; Zheng, X.R.; Zhang, J.; Li, W. Impact of Returning Cotton Stalks to Soil on Residual Film Distribution in Mulched Drip Irrigated Cotton Fields in Typical Oases of Xinjiang. *Agric. Eng. J.* **2018**, *34*, 120–127.
10. Du, L.; Li, Y.N.; Chen, P.P.; Wang, K.; Li, Y. Effects of Different Residue Film Amounts on Soil Environment and Corn Growth. *Water Sav. Irrig.* **2018**, 4–9+14. [CrossRef]
11. Li, Y.Q.; He, W.Q.; Yan, C.R.; Guo, R.; Zhao, C. Effects of Residual Plastic Film on Root Morphology and Physiological Characteristics of Cotton and Corn Seedlings. *J. Agric. Resour. Environ.* **2017**, *34*, 108–114. [CrossRef]
12. Hu, Q.; Li, X.Y.; Shi, H.B.; Chen, N.; Zhang, Y. Effects of Residue Film Pollution on Soil Moisture and Root Growth of Drip Irrigated Corn. *China Environ. Sci.* **2023**, *43*, 5944–5953. [CrossRef]

13. Ya, P.; Hu, Z.C.; You, Z.Y.; Shen, O.; Gu, F.; Wu, F.; Liu, M. Research on the Film-Soil Separation Technology of Shovel-Screen Type Residue Film Recovery Machine. *J. Chin. Agric. Mech.* **2018**, *39*, 21–26. [CrossRef]
14. Chen, X.H.; Chen, X.G.; Li, J.B.; Li, C.; Yang, Y. Design and Experiment of Nail-Tooth Roller Type Residual Film Recovery Device before Sowing. *Agric. Eng. J.* **2020**, *36*, 30–39.
15. Jin, W.; Bai, S.H.; Zhang, X.J.; Zhou, X.; Ma, S. Parameter Optimization and Experiment of the Spring Tooth Residue Film Recovery Machine. *Agric. Mach. Res.* **2020**, *42*, 186–190. [CrossRef]
16. Kang, X.Y.; Zhao, Y.; Chen, X.G.; Zhou, D.X.; Gou, H.X.; Tian, X.L. Design and Experiment of Tooth-Belt Type Residue Film Pickup Mechanism. *J. Gansu Agric. Univ.* **2020**, *55*, 166–174. [CrossRef]
17. Shi, L.L.; Hu, Z.C.; Gu, F.W.; Wu, F.; Chen, Y. Design of Automatic Film Stripping Mechanism for Rake-Type Residue Film Recovery Machine. *Agric. Eng. J.* **2017**, *33*, 11–18.
18. Kang, J.M.; Wang, S.G.; Yan, L.M.; Wang, N.; Di, M.; Du, J. Design and Experiment of Film Lifting Shovel for Residue Film Recovery Machine. *J. Agric. Mach.* **2016**, *47* (Suppl. S1), 143–148.
19. Shi, L.R.; Zhao, W.Y.; Sun, W. Based on Discrete Element Method for Parameter Calibration of Soil Particle Contact Model in Northwest Arid Area. *Agric. Eng. J.* **2017**, *33*, 181–187.
20. Fang, Y.Y.; Zhang, K.P.; Yang, Z.K. Simulation Analysis and Experiment of Plow Tillage Process Based on Discrete Element Method in Northwest Arid Region. *J. Jiangxi Agric. Univ.* **2024**, 1–20. Available online: http://kns.cnki.net/kcms/detail/36.1028.S.20240401.1802.006.html (accessed on 2 April 2024).
21. Li, W.L.; Dai, F.; Zhao, W.Y.; Shi, R.; Song, X.; Ma, H. Simulation Analysis and Experiment of Double-Ridge Seed Bed Tillage and Fertilization Operation Process. *Res. Agric. Arid Areas* **2023**, *41*, 264–273.
22. Zhao, S.H.; Liu, H.P.; Yang, C.; Yang, L.; Gao, L.; Yang, Y. Design and Discrete Element Simulation of Interactive Layered Deep Loosening Shovel for Corn Straw Returning. *J. Agric. Mach.* **2021**, *52*, 75–87.
23. Jin, W.; Ding, Y.C.; Nong, F.; Zhang, X.; Bai, S. Design and Experiment of Jittering Chain Tooth Rod Type Residue Film-Soil-Straw Excavation and Conveying Device. *J. Agric. Mach.* **2023**, *54*, 71–82.
24. Sun, W.; Wang, H.C.; Zhao, W.Y.; Zhang, H.; Liu, X.; Wu, J. Design and Experiment of Residue Film Recovery Type Full-Mulch Covered Potato Digger. *J. Agric. Mach.* **2018**, *49*, 105–114.
25. *GB/T 25412-2021*; Residual Film Recycling Machine. Standards Press of China: Beijing, China, 2021.